

Article

Spatiotemporal Evolution Characteristics of Carbon Emissions from Industrial Land in Anhui Province, China

Ting Zhang ^{1,2}, Longqian Chen ^{1,2,*}, Ziqi Yu ¹ , Jinyu Zang ¹  and Long Li ^{1,2,3} 

¹ School of Public Policy and Management, China University of Mining and Technology, Daxue Road 1, Xuzhou 221116, China

² Research Center for Transformation Development and Rural Revitalization of Resource-Based Cities in China, China University of Mining and Technology, Daxue Road 1, Xuzhou 221116, China

³ Department of Geography, Earth System Sciences, Vrije Universiteit Brussel, Pleinlaan 2, 1050 Brussels, Belgium

* Correspondence: chenlq@cumt.edu.cn; Tel.: +86-516-8359-1327

Abstract: Carbon emissions (CE) in Anhui Province are closely related to carbon emissions from industrial land (CEIL). In this study, based on industrial land, industrial energy consumption, and related statistical data in Anhui Province from 2000 to 2016, the carbon emissions coefficient method and the standard deviational ellipse were used to measure and analyze the CEIL and their spatial and temporal evolution characteristics, aiming to provide a basis for the relevant government departments to formulate CE policies. The main results showed that: (1) The total amount of CEIL followed an inverted U-shaped trend of rapid increase followed by a decrease, while the overall carbon emission intensity from industrial land (CEIIL) followed a downward trend. (2) The CE had an evident spatial differentiation, with those from resource-based cities being much higher than those of industrial and tourism-based cities; (3) The overall pattern of CEIL in Anhui Province showed that the increase in the north-south direction is significantly higher than that in the east-west direction, and mainly expanded in the north-south direction. The overall industrial growth rate of Southern Anhui, represented by the Wanjiang City Belt, was higher than that of Northern Anhui, although its CEIL center showed to move towards Northern Anhui.

Keywords: industrial land; carbon emissions; spatiotemporal evolution; Anhui Province



Citation: Zhang, T.; Chen, L.; Yu, Z.; Zang, J.; Li, L. Spatiotemporal Evolution Characteristics of Carbon Emissions from Industrial Land in Anhui Province, China. *Land* **2022**, *11*, 2084. <https://doi.org/10.3390/land11112084>

Academic Editors: Yanan Wang, Kees Klein Goldewijk, Wei Chen, Juan Wang and Xiaosong Ren

Received: 7 November 2022

Accepted: 16 November 2022

Published: 18 November 2022

Publisher's Note: MDPI stays neutral with regard to jurisdictional claims in published maps and institutional affiliations.



Copyright: © 2022 by the authors. Licensee MDPI, Basel, Switzerland. This article is an open access article distributed under the terms and conditions of the Creative Commons Attribution (CC BY) license (<https://creativecommons.org/licenses/by/4.0/>).

1. Introduction

One of the primary causes of climate change, which is a hazard to the entire planet, is carbon emissions (CE) [1]. Since the industrial revolution, the expansion of human economic activity has increased the need for fossil fuels and dramatically increased the emission of greenhouse gases, which has resulted in sea level rise, glacier melting, and a sharp decline in biodiversity. These effects have put the survival and advancement of human society in severe danger [2,3]. As a significant source of CE, the industrial sector has become the focus of increasing academic attention [4–6]. As countries and the public have become more aware of the dangers of climate warming, a global wave for “energy saving and emission reduction” has emerged [7,8], and the low-carbon economic development model has been adopted by several countries around the world [9].

Typically, methods, including physical measurement, the material balance approach, and the carbon emission coefficients (CEC) method, are used to quantify estimates of industrial CE [10–12]. The actual measurement method is mainly based on continuous monitoring equipment recognized by the relevant authorities for the pollutants to be measured. This method has better reliability and accuracy, but the method is only applicable to the pollutants put into production and is not very operable. Consumption of human, material and financial resources will increase as a result of continual monitoring in the field [13]. The rule of conservation of mass serves as the foundation for the material

balancing technique, which quantifies the CE of materials in industrial production processes. This approach is presently only utilized in a small number of industrial businesses since it requires a significant amount of first-hand production data on industrial production processes [14]. As the CEC for industrial energy is more stable in accordance with IPCC assumptions and can be measured directly in accordance with the CE equations provided by the IPCC for developing countries, the CEC method, which calculates the CE from the consumption of energy, has evolved. The CEC method, with simple data acquisition and easy calculation, is currently a mainstream method for CE measurement and is widely used by scholars [15–19].

In recent years, CE has become one of the hot spots of research, and the research on carbon emissions from industrial land (CEIL) has been gradually deepened [20], and the research on CEIL mainly includes CE performance [21], economic and intensive use of industrial land [22], CE intensity of industrial land [23], and the influence of different land space on CEIL [24], etc., but nowadays, the research mainly focuses on the national or urban clusters, etc. However, the current studies are mainly focused on the national level or city clusters, and there are few studies on the spatial and temporal evolution of CEIL and the characteristics of industrial land. In this paper, we take the Anhui province of China as an example to study the spatial and temporal evolution characteristics of CEIL to provide a basis for industrial land regulation and control policies with the goal of low carbon development.

Anhui province is an underdeveloped province in central China and an important part of the Yangtze River Delta economic belt [25,26]. After full integration into the Yangtze River Delta, Anhui's economy has grown rapidly, with GDP increasing from 123.533 billion yuan in 2010 to 429.592 billion yuan in 2021, with an average annual growth rate of 11.99%, exceeding the national average. On the other hand, Anhui Province is a typical "coal-rich, oil and gas-free" province, where coal has long dominated energy consumption. The rapid progress of industrialization and the consequent CE problems also face serious challenges [27,28]. The 14th Five-Year Plan for Energy Conservation and Emission Reduction promulgated by Anhui Province in 2022 aims to improve the quality of the ecological environment and increase the efficiency of energy utilization. In the plan, it is clear that "to promote high-quality development and comprehensively implement the dual control of energy consumption intensity and total amount." The continuous expansion of Anhui Province's economy and industrial scale has made the contradiction between energy demand expansion and energy conservation, and the task of energy conservation and emission reduction is arduous [29].

Industrial land is the spatial carrier of industrial development. Economic development and CE are closely related to CEIL. This study calculates the CEIL in Anhui Province, analyzes its spatial and temporal evolution characteristics of it, and makes a judgment on the evolution trend of CE, which can provide data support for the decomposition of energy saving and emission reduction targets in different regions and provide a reference for relevant government departments to designate corresponding energy consumption and low carbon development. Secondly, the discussion of CEIL during the accelerated industrialization process in less developed provinces can also provide new ideas and references for the industrial restructuring of regions and provinces with similar background characteristics.

2. Study Area

Anhui Province is located in the middle latitudes of East China (29°41'–34°38' N, 114°54'–119°37' E) (Figure 1); it belongs to the transition zone between the subtropical climate and the warm temperate climate [30]. Anhui Province is split into the Huaibei Plain, South Anhui Plain, and Jianghuai Hills. This province is rich in mineral resources, especially coal resources, while oil and gas resources are limited.

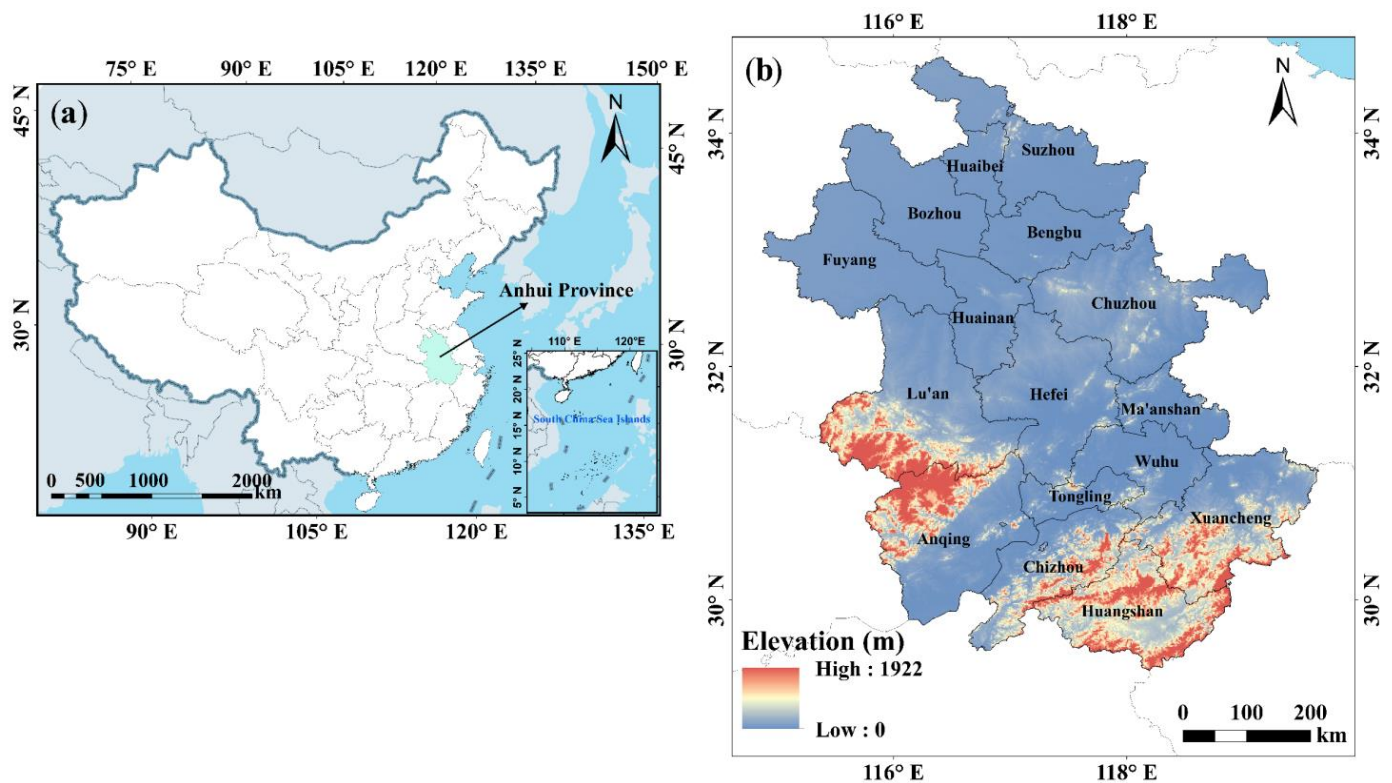


Figure 1. Study area: (a) location of Anhui province in China. (b) geographical map of Anhui province.

3. Materials and Methods

3.1. Data Collection

The socioeconomic statistical data and the energy data of Anhui Province from 2000 to 2016 were mainly derived from the Anhui Statistical Yearbook. The data on the industrial land area of Anhui Province from 2000 to 2016 come from the Statistical Yearbook of China's Urban Construction. Finally, the gross industrial output value (GIOV) by industry of each city was taken from the China Industrial Enterprises Database. Based on the availability of data, the study period about the GIOV by industry of each city was limited from 2000 to 2013.

The administrative division of Chaohu City was adjusted in 2011, and the districts and counties were merged into other cities. In order to ensure the consistency, integrity, and operability of relevant information, the relevant data of Chaohu City from 2000 to 2010 were merged into those of the other cities according to the existing divisions. The vector data were taken from the land use change survey database of Anhui Province in 2016.

3.2. Calculation Methods of Carbon Emissions

In this research, industrial land is defined as the property utilized for manufacturing facilities, storage facilities, and auxiliary infrastructure of industrial and mining businesses, including specialized trains, ports, supplementary roads, and parking lots, but excludes open-pit land. The main emphasis of this definition is on the specific land required for industrial production.

As CO₂ is the main greenhouse gas, CE is usually a general term for, or a synonym of, greenhouse gas emissions [31]. In this study, CE refers to the total amount of direct and indirect greenhouse gas emissions generated by a certain entity within a certain period, represented by carbon [32,33]. CE is mainly divided into renewable energy and non-renewable energy CE. Renewable energy CE is mainly the CE of various biological systems on the earth's surface, including also those generated by various renewable energy utilization processes. Non-renewable energy CE mainly refers to those generated during the combustion of fossil energy [34]. Using fossil fuels for energy is the major source of

industrial CE [35]. Based on previous research, this study defined CEIL as the CE generated by the fossil energy consumed by industrial production in urban areas and industrial land [36–38].

The amount of carbon emitted for every unit of gross industrial production is referred to as industrial carbon emission intensity (ICEI) [39,40]. ICEI can reflect the relationship between CE and industrial development. The formula is as follows:

$$T = \frac{C}{N} \quad (1)$$

where T represents the ICEI, C denotes CE, and N is GIOV.

Carbon emission intensity from industrial land (CEIL) measures the CE per unit of industrial land area. It reflects the CE burden generated by industrial activities across space. The greater the value, the more CE generated by industrial activities on industrial land, and the higher the economic benefits and the environmental burden [41,42]. The formula is as follows:

$$CI = \frac{C}{AI} \quad (2)$$

where CI represents CEIL, C is CE, and the industrial land area is represented by AI [43].

At present, China does not release authoritative data on CE from the industry and its various sectors [44]. In existing studies, national, regional, and sectoral CE data are mostly calculated based on energy consumption and energy CEC. China's industrial CE mainly originates from the consumption of fossil energy [45]. So, in this paper, the CEIL at the provincial level is calculated according to the IPCC-recommended method of estimating energy CEC.

The selected energy consumption includes coal, cleaned coal, liquefied petroleum gas, crude oil, gasoline, kerosene, diesel oil, fuel oil, coke, gas field natural gas, oilfield gas, and coke oven gas. When calculating CE using energy CEC, it is necessary to first convert the physical amount of energy consumption into the standard amount of energy consumption according to the conversion factor of 10,000 tons of standard coal and then multiply by its corresponding energy CEC to obtain [46,47]. The calculation formula was as follows:

$$c_{ji} = \sum_k E_{jki} \times F_k \times M_k \quad (3)$$

$$G_i = \sum_j c_{ji} \quad (4)$$

where c_{ji} indicates the CE of the industrial sector j in the year i ; E_{jki} represents the consumption of fossil fuel k in industrial sector j in the year i ; F_k and M_k are the standard coal conversion coefficient and the CEC, respectively; and G_i indicates the CE of all industrial sectors in a province, namely the CEIL, in the year i . The China Energy Statistical Yearbook's standard coal conversion coefficient was utilized. In this paper, the CEC was adopted following Peng [48], as shown in Table 1.

Due to some incomplete energy data, the CEIL in each city in Anhui Province was measured by using the indirect method [49]. The CE per unit of GIOV was obtained by assessing the CEIL in each province and the GIOV of each industry, on which basis the CEIL in each city was indirectly obtained according to the GIOV of each city, as follows:

$$H_{mi} = \sum_j \frac{c_{ji}}{D_{ji}} a_{mji} \quad (5)$$

where H_{mi} is the CEIL in city m in the year i ; c_{ji} represents the CE of industry j in the year i ; D_{ji} represents the GIOV of industry j in the year i ; and a_{mji} represents the GIOV of industry j in the year i in city m .

Table 1. CEC for each type of fossil energy.

Energy Type	The Standard Coal Conversion Coefficient (kg kg ⁻¹ /kg/m ³)	CEC
Coal	0.7143	0.7599
Cleaned coal	0.9	0.7599
Liquefied petroleum gas	1.7143	0.5042
Crude oil	1.4286	0.5847
Gasoline	1.4714	0.5538
Kerosene	1.4714	0.5714
Diesel oil	1.4571	0.5921
Fuel oil	1.4286	0.6185
Coke	0.9714	0.855
Gas field natural gas	1.2143	0.4483
Oilfield Gas	1.33	0.4483
Coke oven gas	0.5714	0.3548

3.3. Standard Deviation Ellipse Method

Lefever initially presented the standard deviation ellipse (SDE) method in 1926 as a technique for statistically analyzing geographical patterns [50]. It is expressed by shape characteristics, density, distribution, orientation, and centrality, which can objectively reflect the global characteristics of geographical factors in spatial distribution [51]. Currently, it is extensively used in economics, ecology, geology, sociology, and other disciplines [52–55].

The SDE method mainly uses azimuth, short axis, center, and long axis as the basic parameters of a spatial distribution ellipse, to quantitatively reflect the characteristics of the spatial layout of the research object. The elliptical spatial distribution range, where the center reflects the relative positions of the geographical elements in the two-dimensional spatial distribution. The short axis represents the dispersion degree of geographical components in the secondary direction, while the long axis represents the core edge structure of the dispersion degree of geographical elements in the main trend direction [56,57]. The following is the calculation formula for the SDE’s primary parameters:

$$\text{Average center : } \bar{X}_w = \frac{\sum_{i=1}^n w_i x_i}{\sum_{i=1}^n w_i}; \bar{Y}_w = \frac{\sum_{i=1}^n w_i y_i}{\sum_{i=1}^n w_i} \tag{6}$$

$$\text{Azimuth : } \tan\theta = \frac{\left(\sum_{i=1}^n w_i^2 \tilde{x}_i^2 - \sum_{i=1}^n w_i^2 \tilde{y}_i^2\right) + \sqrt{\left(\sum_{i=1}^n w_i^2 \tilde{x}_i^2 - \sum_{i=1}^n w_i^2 \tilde{y}_i^2\right)^2 + 4 \sum_{i=1}^n w_i^2 \tilde{x}_i \tilde{y}_i}}{2 \sum_{i=1}^n w_i^2 \tilde{x}_i \tilde{y}_i} \tag{7}$$

$$\text{x – axis standard deviation : } \sigma_x = \sqrt{\frac{\sum_{i=1}^n (w_i \tilde{x}_i \cos\theta - w_i \tilde{y}_i \sin\theta)^2}{\sum_{i=1}^n w_i^2}} \tag{8}$$

$$\text{y – axis standard deviation : } \sigma_y = \sqrt{\frac{\sum_{i=1}^n (w_i \tilde{x}_i \sin\theta - w_i \tilde{y}_i \cos\theta)^2}{\sum_{i=1}^n w_i^2}} \tag{9}$$

where (x_i, y_i) denotes the spatial location of the object of study; w_i denotes the weight; (\bar{x}_i, \bar{y}_i) denotes the weighted average center; θ is the azimuth angle of the ellipse, indicating the angle formed by the clockwise rotation of the north to the long axis of the ellipse; \tilde{x}_i

and \tilde{y}_i represent the coordinate deviation between the location of each research object to the average center; and σ_x and σ_y represent the standard deviation along the x-axis and y-axis, respectively.

Because the SDE analysis can intuitively reflect the spatial pattern characteristics of geographical elements, this study applied the weighted SDE method in ArcGIS 10.2 software to determine the SDE of each variable in spatial distribution based on the spatial location of each administrative unit of each province and municipality. Moreover, the corresponding CE and industrial variable indicators were used to represent the weight, and the ArcGIS 10.2 spatial statistical module was employed to calculate the parameters and create spatial visualization. In this way, the SDE parameters of GIOV and CEIL in Anhui Province from 2000 to 2013 were obtained, reflecting the spatial distribution pattern changes of different factors according to the standard deviation of the long and short axes, the location of the center point, and the specific movement and shape index.

4. Results and Discussion

4.1. Evolution Characteristics at the Provincial Level

At the provincial level, CEIL and GIOV in Anhui Province had an overall growth trend (Figure 2), although the growth rate of the former was significantly lower than that of the latter. For example, the GIOV increased from 166.144 billion yuan in 2000 to 434.3635 billion yuan in 2016, with an average annual growth of 12.26%. In the same years, the CEIL increased from 262.2284 Mt to 1122.974 Mt, an average annual increase of 9.51%. In addition, under the condition that the growth rate of GIOV was stable, the CEIL in Anhui Province showed an inverted U-trend of rapid increase followed by a gradual decrease (Figure 3). Anhui Province has achieved some achievements in promoting the transformation of the economic development model and industrial low-carbon transformation during the 12th five-year plan.

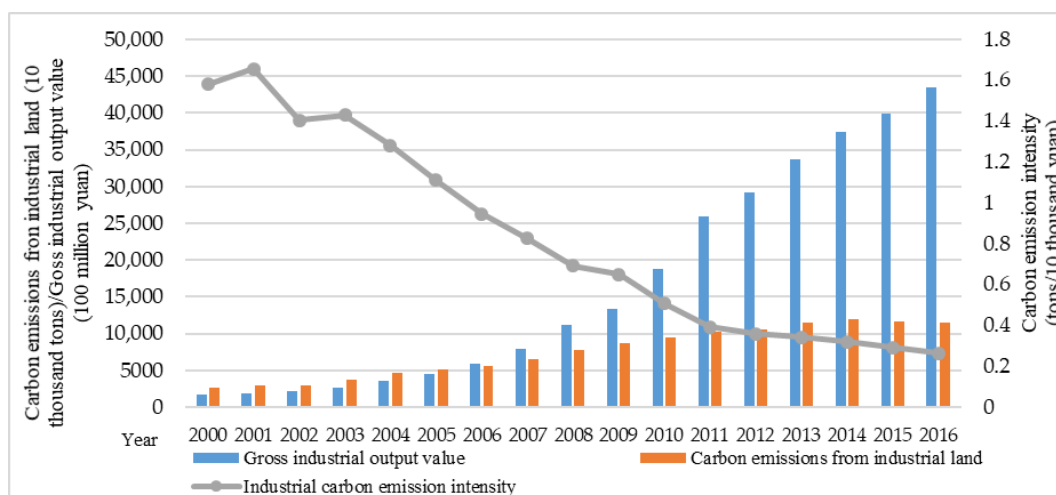


Figure 2. Changes in CEIL, GIOV, and ICEI in Anhui Province from 2000 to 2016.

4.1.1. Relationship between CEIL and Economic Development

During the research phase, the value of CE per unit of GIOV first increased and then decreased from 1.58 tons per million yuan in 2000 to 0.39 tons per million yuan in 2012, i.e., less than 1/3 of the original value, after which the decline began to slow down, finally reaching 0.26 tons per million yuan in 2016 (Figure 2).

Meanwhile, the GDP per capita of Anhui Province increased from 4779.46 yuan per person in 2000 to 39091.81 yuan per person in 2016. Anhui Province's GDP per capita and CEIL showed a clear exponential positive correlation (Figure 4), and it still did not reach its peak in 2016, indicating that economic growth is the main driving force for carbon emission growth.

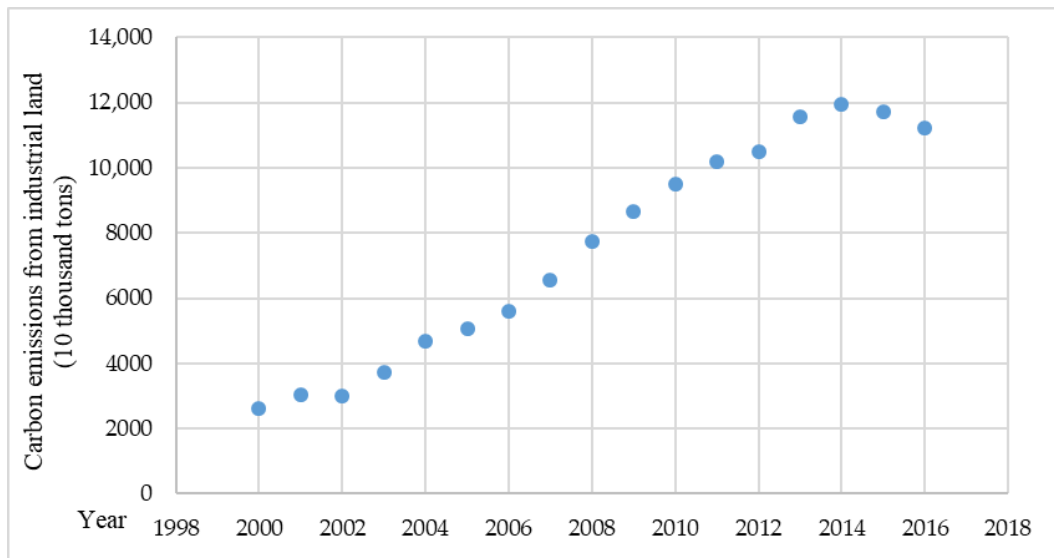


Figure 3. CEIL in Anhui Province from 2000 to 2016.

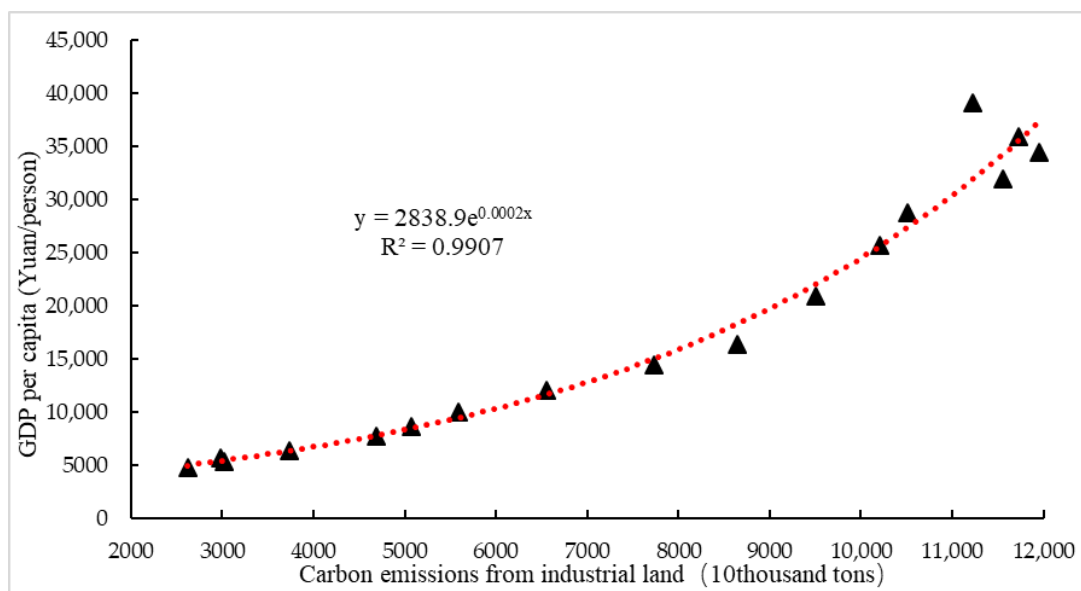


Figure 4. Relationship between CEIL and GDP per capita in Anhui Province from 2000 to 2016.

4.1.2. Time Series Relationship between CEIL and Structure of Energy Consumption

From the analysis of the industrial energy consumption structure (Table 2), it can be found that the CEIL from coal consumption was the highest during the study period. This indicates evident structural problems in industrial energy consumption in Anhui Province, the proportion of clean oil and natural gas consumption was too low.

Table 2. The proportion of CEIL from the consumption of various types of fossil energy in Anhui Province in 2000 and 2016.

Type (%)	2000 (%)	2016 (%)
CEIL from raw coal	69.55	80.16
CEIL from crude oil	10.98	4.02
CEIL from natural gas	0.00	0.06
CEIL from other energy sources	19.47	15.76

4.2. Evolution Characteristics at the City Level

4.2.1. Spatiotemporal Characteristics of CEIL

CEIL in Anhui Province was found to have a clear spatial differentiation. Figure 5 shows the CEIL in each city in 2000 and 2013, from which it can be seen that the CEIL in resource-based cities are significantly larger than those in industrial and tourism-based cities (Resource-based cities refer to those cities with mining and processing of natural resources such as minerals and forests in the region as the leading industry, industrial cities refer to those cities with industry as the pillar industry, and tourism-based cities refer to those cities with unique tourism resources and cultural tourism industry as the main industry [58]. Typical resource-based cities in Anhui Province include Huainan, Ma'anshan, and Huaibei; typical industrial cities include Hefei, Wuhu, and Anqing, and typical tourism-based cities include Huangshan [59,60]). For example, Huainan had the highest level of CEIL among all cities in the province throughout the whole study period, followed by Huaibei and Ma'anshan. On the contrary, Huangshan, whose economy is predominantly based on tourism, had the lowest level of CEIL.

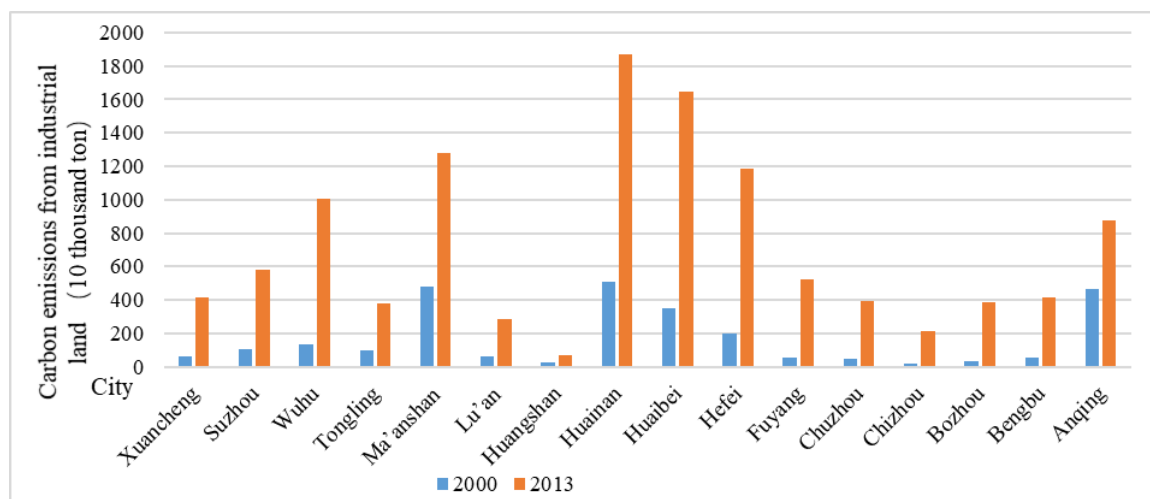


Figure 5. CEIL in 16 prefectural cities in Anhui Province in 2000 and 2013.

Overall, during the period 2000–2013, the CEIL of 16 prefecture-level cities had an increasing trend; in particular, this growth trend was highest in Bozhou and Chizhou (i.e., more than 20% annually) and lowest in Ma'anshan, Huangshan, and Anqing (i.e., less than 10%).

From 2000 to 2013, among the changes in the growth rate of CEIL in 16 cities in Anhui Province, only Ma'anshan City showed a polynomial growth trend, reaching a maximum in 2008, and then began to decline (Figure 6b). In parallel, the CEIL of Anqing, Xuancheng, Tongling, Huangshan, and Hefei followed a linear growth trend (Figure 6a). A total of 10 cities recorded exponential growth in CEIL, following an accelerating upward trend (Figure 6c). On this premise, it is possible to forecast that Anhui Province's industrial land will continue to produce more carbon dioxide overall in the future.

4.2.2. Spatiotemporal Characteristics of ICEI

During the research phase, the ICEI of 16 prefecture-level cities in Anhui Province declined continuously, although the performance was not the same across cities. The ICEI in Anqing, Suzhou, Ma'anshan, Huaibei, and Huainan was higher than the provincial average in 2000, and the ICEI in Suzhou, Bozhou, Ma'anshan, Huaibei and Huainan was higher than the provincial average in 2013. See Table 3.

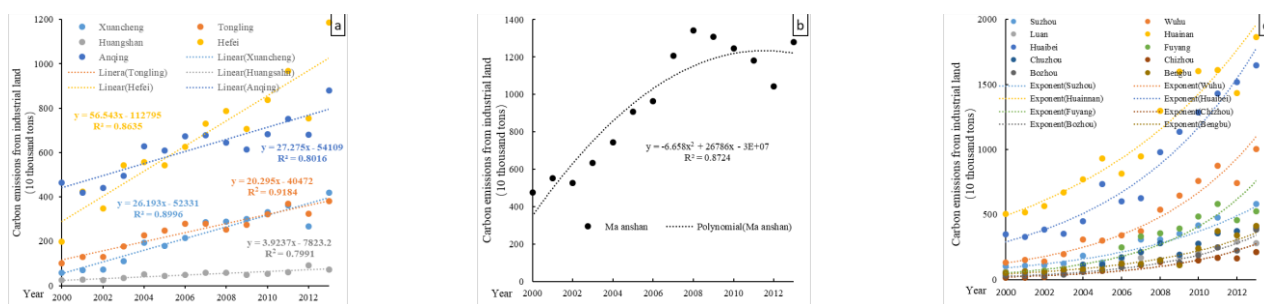


Figure 6. Changes in CEIL in 16 prefectural cities in Anhui Province from 2000 to 2013: (a) a linear growth trend; (b) a polynomial growth trend; and (c) an exponential growth trend.

Table 3. Changes in the ICEI of prefecture-level cities in Anhui Province from 2000 to 2013. Unit: ton/ten thousand yuan.

City	2000	2001	2002	2003	2004	2005	2006	2007	2008	2009	2010	2011	2012	2013
Huangshan	0.95	0.95	0.78	0.85	0.96	0.60	0.48	0.38	0.28	0.21	0.16	0.14	0.20	0.14
Hefei	0.59	1.06	0.70	0.91	0.70	0.58	0.53	0.46	0.29	0.23	0.19	0.16	0.10	0.14
Lu'an	0.83	0.82	0.90	1.02	0.95	0.71	0.67	0.53	0.34	0.31	0.26	0.22	0.21	0.18
Chuzhou	0.39	0.43	0.35	0.42	0.54	0.45	0.52	0.48	0.48	0.27	0.26	0.23	0.22	0.20
Wuhu	0.80	0.73	0.53	0.54	0.60	0.48	0.39	0.33	0.36	0.35	0.29	0.24	0.17	0.21
Tongling	1.11	1.36	1.22	1.22	1.02	0.80	0.57	0.47	0.38	0.42	0.29	0.24	0.20	0.21
Bengbu	0.60	0.66	0.55	0.60	0.46	0.37	0.46	0.36	0.40	0.20	0.31	0.29	0.23	0.23
Xuancheng	0.79	0.88	0.84	1.02	1.22	0.90	0.71	0.65	0.49	0.40	0.31	0.26	0.21	0.28
Anqing	2.49	2.39	2.33	2.20	2.11	1.72	1.48	1.11	0.83	0.63	0.52	0.41	0.32	0.34
Chizhou	1.01	1.00	0.98	1.52	1.49	1.33	1.42	1.23	0.91	0.62	0.49	0.45	0.34	0.38
Fuyang	0.74	0.92	0.88	0.89	0.78	0.72	1.19	1.10	0.91	0.76	0.69	0.63	0.43	0.39
Suzhou	2.58	2.57	2.46	2.69	2.41	1.30	1.12	1.41	0.87	0.73	0.61	0.41	0.40	0.48
Bozhou	0.66	0.84	0.81	0.84	0.90	0.90	0.94	0.87	0.80	0.54	0.58	0.47	0.36	0.52
Ma'anshan	3.27	3.26	2.64	2.29	1.71	1.59	1.51	1.30	1.07	1.03	0.85	0.66	0.52	0.54
Huaibei	4.28	3.51	3.55	2.91	2.47	3.28	2.51	2.09	2.05	1.93	1.46	1.19	1.04	1.01
Huainan	5.20	4.85	4.26	4.36	3.49	3.33	2.67	2.72	2.34	2.45	2.03	1.80	1.44	1.73
Average	1.64	1.64	1.49	1.52	1.36	1.19	1.07	0.97	0.80	0.69	0.58	0.49	0.40	0.44

By analyzing the dynamic change characteristics of ICEI from 2000 to 2013, it was possible to classify the 16 prefecture-level cities in Anhui Province into three groups: cities with a stable decrease, cities with a first increase followed by a decrease, and cities with a “fast-slow” decrease.

(1) Cities with a stable decrease

This group includes cities such as Anqing, Ma'anshan, Lu'an, Tongling, Suzhou, Huaibei, and Huainan, characterized by the fact that the ICEI has always been higher than the average of the whole province during the whole study period. This, in turn, indicates a large room for the decline, which indeed took place steadily since 2000 (Figure 7a).

(2) Cities with a first increase followed by a decrease

Chuzhou, Xuancheng, Chizhou, Fuyang, and Bozhou are the representative cities of this group, where ICEI increased first, generally reaching the highest value in 2005–2006, after which they began to decline and stabilize (Figure 7b).

(3) Cities with a “fast-slow” decrease (exponential convergence)

This group includes cities such as Huangshan, Hefei, Wuhu, and Bengbu, characterized by a level of ICEI that was the lowest in the whole province and by an exponential downward trend during the study period. In the first half of the study period, the decline rate was relatively high, with a turning point generally observed from 2006 to 2008, after which the decline rate gradually slowed down and stabilized (Figure 7c).

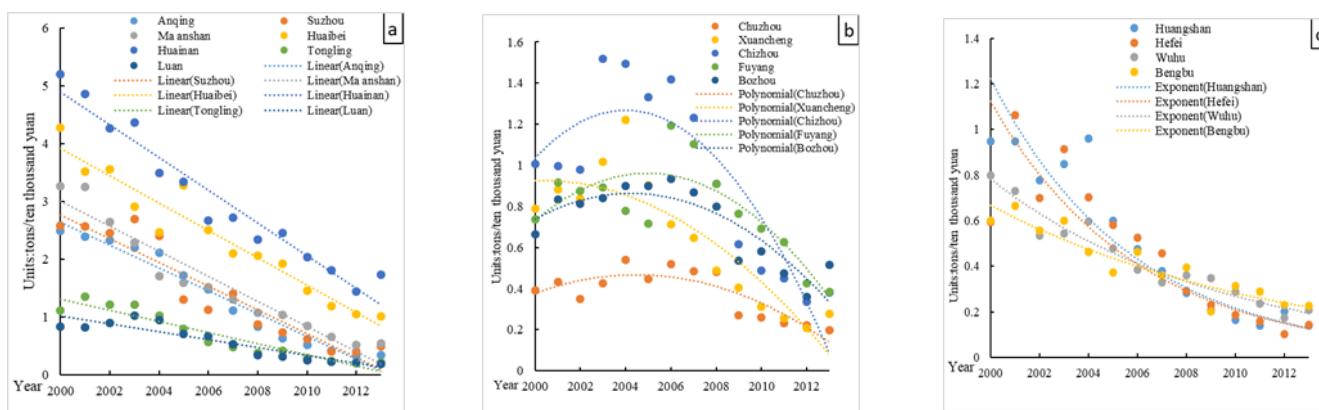


Figure 7. Classification of the 16 prefectural cities of Anhui Province according to their ICEI from 2000 to 2013: (a) cities with a stable decrease; (b) cities with a first increase followed by a decrease; and (c) cities with a “fast-slow” decrease (exponential convergence).

This group includes cities such as Huangshan, Hefei, Wuhu, and Bengbu, characterized by a level of ICEI that was the lowest in the whole province and by an exponential downward trend during the study period. In the first half of the study period, the decline rate was relatively high, with a turning point generally observed from 2006 to 2008, after which the decline rate gradually slowed down and stabilized.

4.2.3. Spatial and Temporal Characteristics of CEIIL

CEIIL is mainly related to the efficiency of land use intensity and the concentration of different industrial sectors. Table 4 demonstrates that in 2000 the CEIIL exceeded the provincial average in Anqing, Ma’anshan, Huainan, and Huaibei, while in 2013, it exceeded the provincial average in Wuhu, Suzhou, Chizhou, Huainan, and Huaibei.

Table 4. Changes in the CEIIL of prefecture-level cities in Anhui Province from 2000 to 2013. Unit: 10 thousand tons /km².

City	2000	2001	2002	2003	2004	2005	2006	2007	2008	2009	2010	2011	2012	2013
Hefei	6.10	13.01	9.63	15.03	15.26	10.23	12.37	14.36	14.41	12.53	12.18	12.50	10.49	15.89
Wuhu	9.21	10.39	7.22	9.72	14.59	13.37	12.96	14.25	20.52	24.47	28.39	31.23	57.17	77.16
Bengbu	6.07	7.39	7.12	9.36	5.11	4.88	7.40	5.80	6.76	5.18	11.38	19.18	16.07	17.95
Huainan	24.03	24.43	26.62	33.54	38.45	44.00	37.61	42.91	57.60	70.29	103.54	103.91	95.70	111.16
Ma’anshan	30.11	33.98	29.07	29.94	34.16	40.71	40.93	50.52	50.34	46.72	41.99	38.12	49.83	33.46
Huaibei	38.83	36.27	38.96	35.89	45.50	53.54	51.34	46.13	62.03	65.22	67.30	73.58	75.89	82.25
Tongling	11.10	14.01	14.15	19.25	24.84	25.57	30.52	30.57	27.10	29.45	34.54	39.63	32.67	29.00
Anqing	26.78	24.07	25.10	25.77	28.15	23.96	28.25	24.95	21.97	19.85	21.37	21.96	19.79	25.59
Huangshan	5.69	7.54	6.15	8.99	15.55	10.48	14.65	16.44	10.10	8.47	9.10	8.27	12.18	8.64
Chuzhou	4.20	4.93	4.34	5.98	9.82	6.48	8.36	8.02	9.97	6.12	8.12	9.91	12.38	11.81
Fuyang	7.75	8.86	8.32	9.92	7.41	10.20	23.56	31.53	31.50	34.49	42.40	38.23	32.04	34.37
Suzhou	7.53	7.32	7.63	8.54	12.39	8.46	18.85	34.41	29.97	28.76	31.52	35.37	24.89	40.15
Lu’an	5.61	5.76	6.27	7.52	12.13	11.41	15.19	17.04	13.95	15.95	17.64	20.34	23.16	21.67
Bozhou	4.91	5.00	4.91	5.98	8.90	10.68	14.42	17.20	19.14	16.50	23.74	20.07	17.25	29.80
Chizhou	6.73	6.84	8.54	19.09	21.30	20.47	24.50	22.74	27.73	31.25	27.61	31.68	37.06	47.16
Xuancheng	12.97	13.52	12.93	18.56	27.73	21.26	24.54	30.69	26.45	23.32	21.40	22.84	11.75	17.91

The 16 cities under investigation were divided into three groups based on an examination of the features of the dynamic changes in the CEIIL in Anhui Province between 2000 and 2013 (Figure 8):

(1) Cities with a continuous increase

This group includes eight cities, namely Lu’an, Fuyang, Chizhou, Huaibei, Bozhou, Suzhou, Wuhu, and Huainan, where the CEIIL continuously increased during the study period (Figure 8a). More in detail, the increased rate of CEIIL in Huainan and Huaibei was significantly higher than in other cities, mainly because these are coal resource-based cities, and the industries include mainly mining and heavy chemical industries. In addition, the

intensive use of industrial land in these cities is generally not high, which is also one of the reasons for the high CEIL.

(2) Cities with a first increase followed by a decrease

This group includes the cities of Huangshan, Xuancheng, Anqing, Tongling, and Ma'anshan (Figure 8b), which are all located along the Yangtze River and are characterized by a yearly increase in the degree of industrial land intensity. In these cities, the CEIL increased rapidly, at first reaching a peak in 2006–2008 and then gradually decreasing. Among these cities, the ICEI and CEIL of Huangshan City were the lowest in the whole province, mainly because this is a tourist city and hosts relatively few industries.

(3) Cities with fluctuating increase

This group includes the cities of Chuzhou, Hefei, and Bengbu (Figure 8c), where the CEIL fluctuated greatly from 2000–2013, following an overall upward trend.

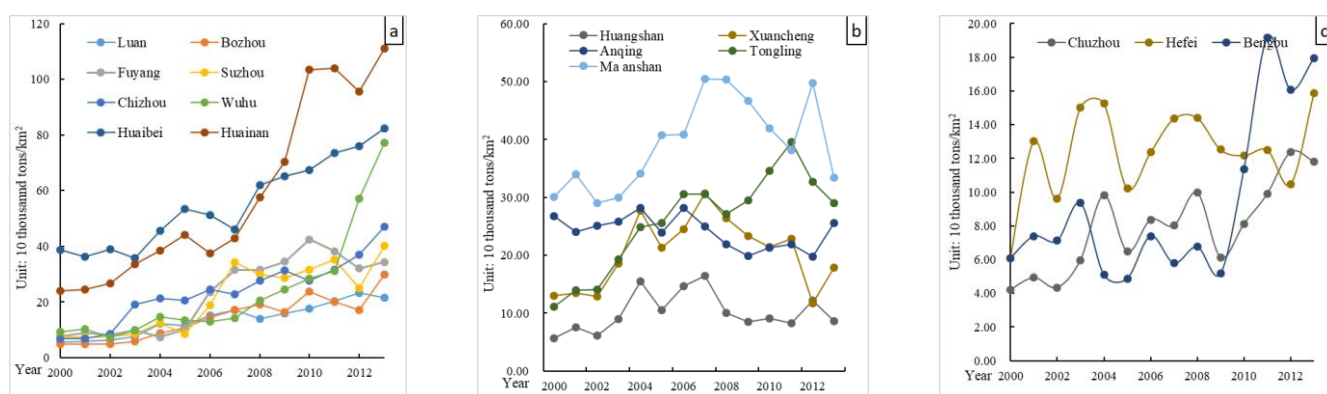


Figure 8. Changes in CEIL of 16 prefectural cities in Anhui Province from 2000 to 2013: (a) cities with a continuous increase; (b) cities with a first increase followed by a decrease; and (c) cities with fluctuating increase.

4.3. A Comprehensive Analysis of Evolution Characteristics

4.3.1. Spatial Distribution Features

According to Tables 5 and 6 and Figures 9 and 10, the geographical distribution of CEIL in Anhui Province is mostly defined by a northwest-southeast trend, showing a significant increase in the x-axis direction from 368.46 km in 2000 to 373.05 km in 2013 and a downward trend along the y-axis direction from 173.93 km in 2000 to 157.27 km in 2013. This indicates that the increase in CEIL in Anhui Province from 2000–2013 was significantly higher in the NS direction than that in the EW direction. The spatial pattern of CEIL was mainly a north-south expansion. From the comparative analysis of the SDE (Figure 9) of CEIL and GIOV, both consistency and differences in spatial distribution were observed among these two.

The consistency is manifested in the northwest-southeast pattern, while the differences are manifested in the spatial distribution of the SDE of the GIOV in Anhui Province, which is mainly close to the northeast region. The length of the long axis of the ellipse was smaller than that of the long axis of CEIL, although the length of the short axis was significantly larger than that of the short axis of CEIL. This clearly shows the spatial differentiation and spatial aggregation characteristics of the GIOV and its CEIL and reflects the fact that the spatial dispersion of the GIOV in Anhui Province was significantly smaller than that of the CEIL. It can also be seen from Figure 9 that the regions with the rapid growth of GIOV in Anhui Province were mainly located in Southern Anhui and Northern Anhui, which indicates that the CEIL in Anhui Province was mainly related to the rapid growth of the industrial sector. However, by comparing the shape index of the two (Figure 10), it can be found that the shape index of CEIL was significantly lower than that of the GIOV.

Table 5. Standard deviation ellipse parameters of GIOV in Anhui Province from 2000 to 2013.

Year	Length Along the X-Axis (km)	Length Along the Y-Axis (km)	Corner $\theta/^\circ$	Shape Index	Center Point Longitude	Center Point Latitude	Center Point Travel Distance (km)
2000	332.5648	185.9253	148.8502	0.5591	117.4815	31.87549	-
2001	329.8621	184.5526	149.3329	0.5595	117.503	31.87627	2.0063
2002	316.7730	179.3950	148.3463	0.5663	117.5082	31.91052	3.8854
2003	332.1035	177.4020	148.4271	0.5342	117.5287	31.90536	2.0018
2004	297.4051	179.1823	146.5859	0.6025	117.5613	31.74423	18.3888
2005	305.7318	204.8776	145.7331	0.6701	117.629	31.73695	6.3682
2006	325.2200	200.8603	140.3168	0.6176	117.5295	31.72676	9.3542
2007	319.1689	201.2809	146.4969	0.6306	117.6355	31.64998	13.1403
2008	350.0887	195.8500	147.7696	0.5594	117.5267	31.89085	28.9476
2009	376.3077	206.4175	149.7956	0.5485	117.5371	31.85602	4.0383
2010	339.9784	192.1851	158.3078	0.5653	117.4205	31.67886	22.7152
2011	339.5637	192.7145	150.1284	0.5675	117.4669	31.84986	19.7251
2012	315.5482	184.7639	148.6076	0.5855	117.4183	31.85691	4.5960
2013	354.6385	194.8166	149.1212	0.5493	117.4523	32.01192	17.7341

Table 6. Standard deviation ellipse parameters of CEIL in Anhui Province from 2000 to 2013.

Year	Length Along the X-Axis (km)	Length Along the Y-Axis (km)	Shape Index	Corner $\theta/^\circ$	Center Point Longitude	Center Point Latitude	Center Point Travel Distance (km)
2000	368.4625	173.9290	0.4720	158.2997	117.4290	32.0134	-
2001	359.9858	172.5175	0.4792	155.9261	117.4780	32.0405	5.5235
2002	350.1577	170.7132	0.4875	156.5649	117.4570	31.9960	5.3978
2003	359.4039	169.6379	0.4720	155.1829	117.4890	32.0213	4.1235
2004	349.7740	170.0246	0.4861	155.3808	117.5170	31.9387	9.6706
2005	361.6847	165.0617	0.4564	155.1621	117.5020	32.0146	8.6744
2006	361.5075	174.9090	0.4838	155.0922	117.4820	32.0324	2.7294
2007	362.6224	175.1150	0.4829	152.6779	117.4820	32.0812	5.4922
2008	355.7807	164.1931	0.4615	151.1164	117.4500	32.1585	9.1917
2009	360.0115	158.2403	0.4395	151.4397	117.4200	32.2541	11.1228
2010	364.2466	159.3147	0.4374	152.4104	117.3960	32.2713	2.9744
2011	368.4817	160.3891	0.4353	153.3811	117.3680	32.3015	4.2475
2012	370.0547	158.7944	0.4291	153.4240	117.3760	32.2852	1.9519
2013	373.0478	157.2671	0.4216	153.6727	117.3480	32.3169	4.4103

Note: Shape index = y-axis standard deviation/x-axis standard deviation.

The shape index of GIOV was relatively stable, except for the period 2004–2007, when it increased to more than 0.6, after which it declined slowly and was around 0.5. In addition to being significantly lower than the shape index of GIOV, the shape index of CEIL also showed a downward trend year by year, from 0.47 in 2000 to 0.42 in 2013. In parallel with the decline of the shape index of GIOV, the shape index of CEIL after 2013 followed a continuous downward trend. This indicates that the spatial dispersion of CEIL in Anhui Province strengthened, and its CEIL increment was mainly concentrated in the northwest and southeast endpoints (i.e., Northern and Southern Anhui). Although the overall industrial growth rate in south Anhui, represented by the Wanjiang City Belt, was higher than that in north Anhui, its CEIL center was found to move towards north Anhui.

4.3.2. Center Change Feature

Hefei (Feidong County—Changfeng County) was the location of the spatial pattern of CEIL in Anhui Province throughout the research period, which was consistent with its geographical and economic center (Figure 11). It moved from the northeast (2000–2002) to the southeast (2002–2004) and then to the northwest (2004–2013), showing an overall direction south-east-northwest. From the point of view of the movement rate, a serrated and unstable change trend was observed, and the average movement distance was 5.81 km/year.

During the 10th Five-Year Plan period, the center position was generally located at the junction of Feidong County and Changfeng County; however, its location was not stable, and the Center gradually changed from the northeast to the southeast. The movement rate was slow at first and then accelerated, reaching 9.67 km from 2003 to 2004. Since the 11th Five-Year Plan, the migration direction of the center was reversed by 180° and moved from the southeast to the northwest; the movement rate significantly accelerated, with an average rate of 7.44 km/year, and the center reached the first Changfeng County in 2010. During the 12th Five-Year Plan period, the center moved stably in the northwest direction and continued to penetrate the hinterland of Changfeng County, although the movement rate slowed to 3.40 km/year.

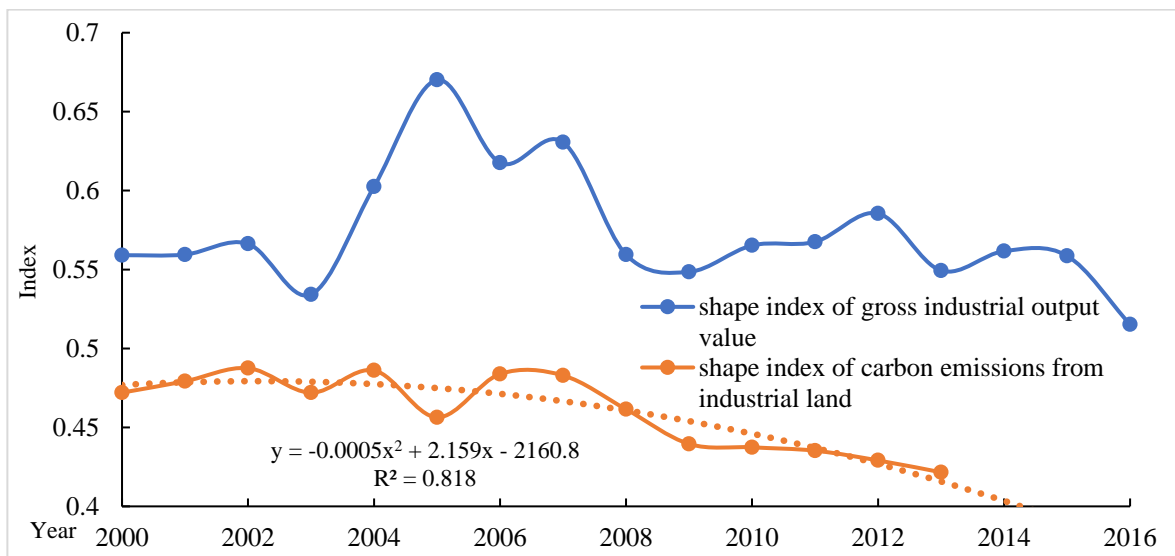


Figure 9. Comparison of the standard deviation ellipse shape indices of GIOV and CEIL in Anhui Province from 2000 to 2016.

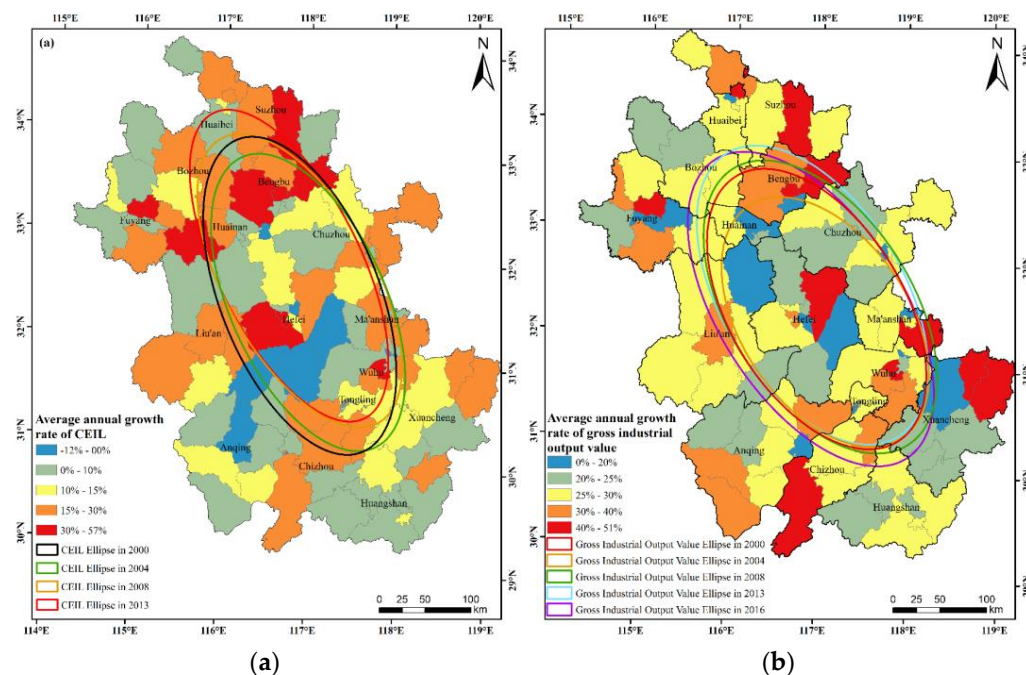


Figure 10. Comparison of the standard deviation ellipses of GIOV and CEIL in Anhui Province: (a) CEIL standard deviation ellipse; (b) GIOV standard deviation ellipse.

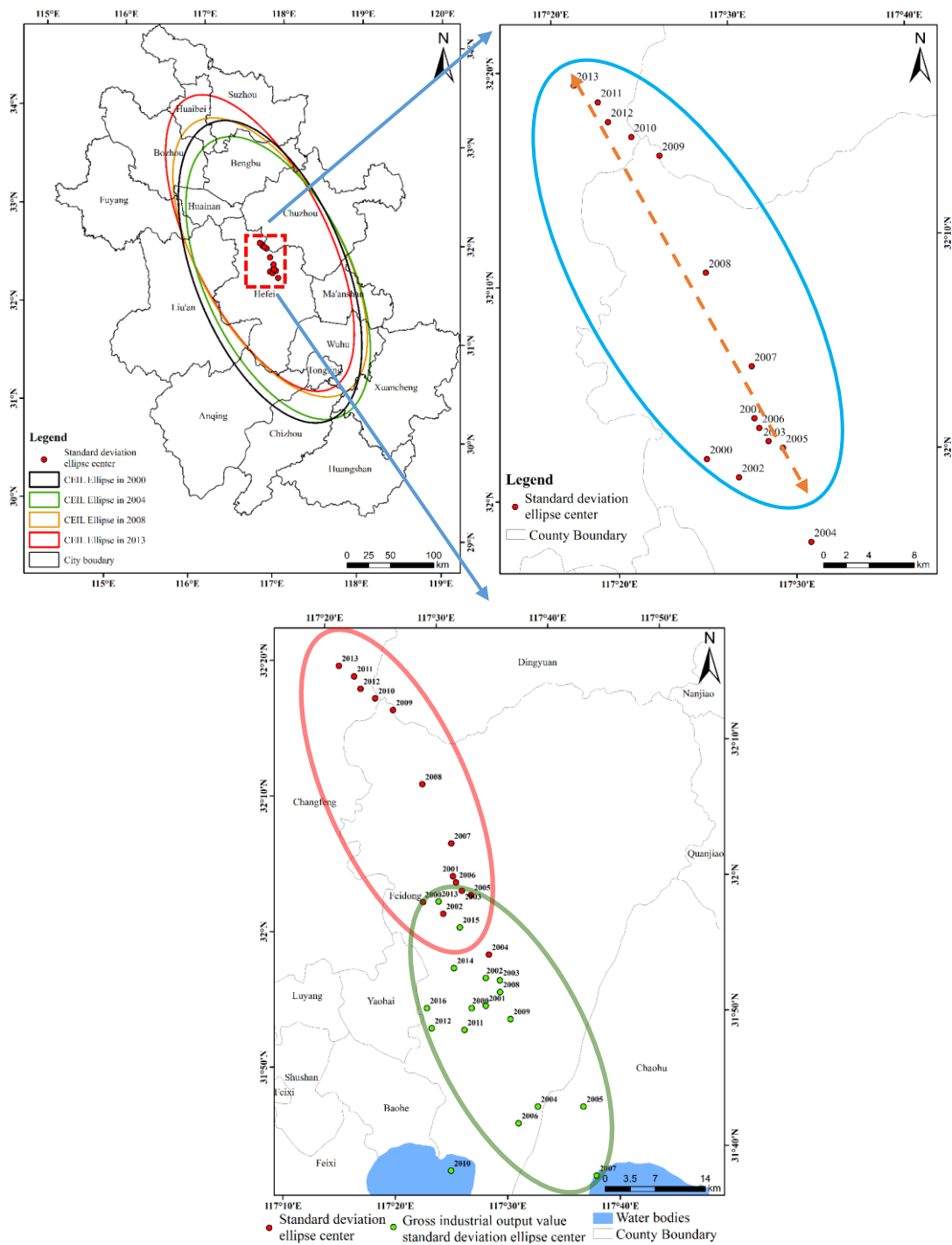


Figure 11. Positional changes in the elliptical center points of GIOV and CEIL standard in Anhui Province from 2000 to 2013.

Compared with the movement of the center of GIOV, it can be found that:

- (1) The movement trend of the center of CEIL was consistent with that of the industrial sector, although the scope and extent of the latter were larger and more dispersed, and the industrial center was more oriented towards the southeast. In particular, from 2004 to 2007, Anhui’s industrial center moved significantly to the southeast, reaching Chaohu, mainly due to the transfer of a large number of manufacturing industries from the Yangtze River Delta to Anhui Province during this period, particularly to the Wanjiang urban belt area. After 2008, with the implementation of the “Rise of Central

China” Plan and the rapid rise of Hefei, its industrial center began to move to the northwest and gradually stabilized in Hefei.

- (2) The movement trend and the rate of the CEIL center were consistent with, although lower than, those of the industrial center, indicating that CE followed industrial development (Figure 12).

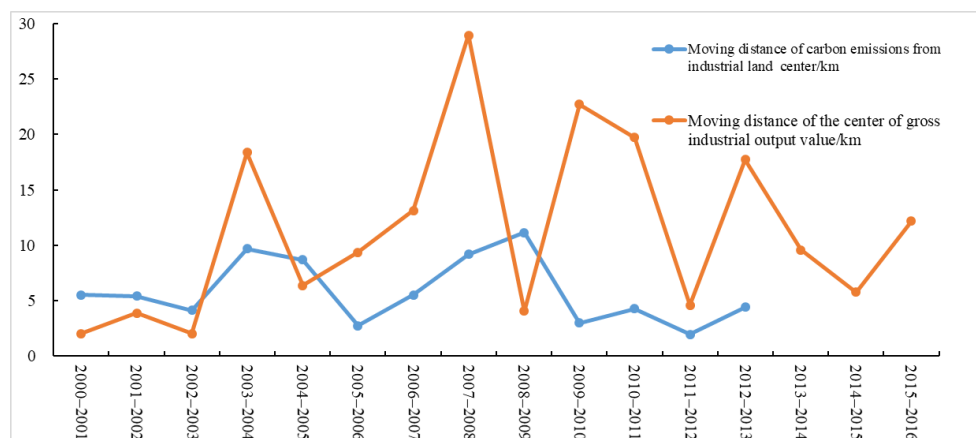


Figure 12. Comparison of the movement rates of the standard deviation ellipses of the GIOV center and CEIL center in Anhui Province from 2000 to 2016.

4.3.3. Spatial Rotation Angle Change

During the study period, the rotation angle θ of the GIOV remained stable between 147° – 148° , while that of CEIL was between 153.67° and 158.30° . The specific analysis showed that, although the main axis direction of CEIL was always northwest-southeast, the rotation angle decreased year by year, and there was a trend of northward rotation. Although the rotation angle decreased, the decrease was small, demonstrating a persistent geographical pattern of CEIL in the province of Anhui.

5. Conclusions

This study assessed the spatial and temporal evolution characteristics of CEIL in Anhui Province from the perspectives of CE, CE intensity, and CE center, reaching the following conclusions.

- (1) The CEIL in Anhui Province from 2000 to 2016 followed an inverted U-shaped trend of rapid increase at first, followed by a decrease, while the overall CEIL showed to follow a downward trend. This shows that Anhui Province has achieved some progress in promoting the transformation of its economic development model and industrial low-carbon transformation during the 12th five-year Plan period, and the rapid growth momentum of CE has been curbed to some extent.
- (2) At the city level, the spatial differentiation of CEIL in Anhui Province is obvious, with those from resource-based cities being much higher than those from industrial and tourism-based cities. Based on their ICEIL, the 16 cities in Anhui Province were divided into three types: cities with a stable decrease, cities with a first increase followed by a decrease, and cities with a “fast-slow” decrease. In parallel, depending on their CEILI, the 16 cities were divided into three types: cities with a continuous increase, cities with a first increase followed by a decrease, and cities with a fluctuating increase.
- (3) The overall CEIL spatial pattern of industrial land in Anhui Province was characterized by the fact that the increase in the north-south direction was significantly higher than that in the east-west direction. The overall industrial growth rate of Southern Anhui, represented by the Wanjiang City Belt, was higher than that of Northern Anhui, although its CEIL center showed to move towards Northern Anhui.

In this paper, the accounting of CEIL mainly adopts the CEC method, which mainly considers CE from fossil energy consumption of industrial production. In the future, for CE from industrial production processes, field monitoring of CE from micro-enterprises can be considered and based on the results of long-term field monitoring, a database of CEIL of enterprises in different industries can be established, thus enhancing the actual measurement of CEIL research data.

Author Contributions: T.Z.: Conceptualization, Formal analysis, Methodology, Writing—Original draft. L.C.: Conceptualization, Funding acquisition, Supervision, Writing—Review, and editing. Z.Y.: Investigation, Visualization, Writing—Original draft. J.Z.: Visualization, Writing—Original draft. L.L.: Investigation, Writing—Review, and editing. All authors have read and agreed to the published version of the manuscript.

Funding: This research was supported by the Fundamental Research Funds for the Central Universities (Grant No.: 2018ZDPY07), the Graduate Innovation Program of China University of Mining and Technology (2022WLKXJ093) and the Postgraduate Research & Practice Innovation Program of Jiangsu Province (KYCX22_2474).

Institutional Review Board Statement: Not applicable for this study.

Informed Consent Statement: Not applicable for this study.

Data Availability Statement: Not applicable.

Conflicts of Interest: The authors declare no conflict of interest.

References

1. Nema, P.; Nema, S.; Roy, P. An overview of global climate changing in current scenario and mitigation action. *Renew. Sustain. Energy Rev.* **2012**, *16*, 2329–2336. [[CrossRef](#)]
2. Ma, Z.W.; Yan, Y.X.; Wu, R.T.; Li, F.X. Research on the correlation between WTI crude oil futures price and European carbon futures price. *Front. Energy Res.* **2021**, *9*, 735665. [[CrossRef](#)]
3. Adnan, M.N.; Safeer, R.; Rashid, A. Consumption based approach of carbon footprint analysis in urban slum and non-slum areas of Rawalpindi. *Habitat Int.* **2018**, *73*, 16–24. [[CrossRef](#)]
4. Ma, X.; Jiang, P.; Jiang, Q. Research and application of association rule algorithm and an optimized grey model in carbon emissions forecasting. *Technol. Forecast. Soc. Change* **2020**, *158*, 120159. [[CrossRef](#)]
5. Gao, P.; Yue, S.; Chen, H. Carbon emission efficiency of China's industry sectors: From the perspective of embodied carbon emissions. *J. Clean. Prod.* **2021**, *283*, 124655. [[CrossRef](#)]
6. Martins, T.; Barreto, A.C.; Souza, F.M.; Souza, A.M. Fossil fuels consumption and carbon dioxide emissions in G7 countries: Empirical evidence from ARDL bounds testing approach. *Environ. Pollut.* **2021**, *291*, 118093. [[CrossRef](#)]
7. Shen, W.; Liang, H.; Dong, L.; Ren, J.; Wang, G. Synergistic CO₂ reduction effects in Chinese urban agglomerations: Perspectives from social network analysis. *Sci. Total Environ.* **2021**, *798*, 149352. [[CrossRef](#)] [[PubMed](#)]
8. Zhang, D.H.; Zhou, C.S.; He, B.J. Spatial and temporal heterogeneity of urban land area and PM_{2.5} concentration in China. *Urban Clim.* **2022**, *45*, 101268. [[CrossRef](#)]
9. Song, C.R.; Yang, J.; Wu, F.; Xiao, X.M.; Xia, J.H.; Li, X.M. Response characteristics and influencing factors of carbon emissions and land surface temperature in Guangdong Province, China. *Urban Clim.* **2022**, *46*, 101330. [[CrossRef](#)]
10. Yang, Y.; Yang, S. Are industrial carbon emissions allocations in developing regions equitable? A case study of the northwestern provinces in China. *J. Environ. Manag.* **2020**, *265*, 110518. [[CrossRef](#)]
11. Pang, Q.; Zhou, W.; Zhao, T.; Zhang, L. Impact of urbanization and industrial structure on carbon emissions: Evidence from Huaihe River Eco-Economic Zone. *Land* **2021**, *10*, 1130. [[CrossRef](#)]
12. Yang, Y.; Yuan, Z.; Yang, S. Difference in the drivers of industrial carbon emission costs determines the diverse policies in middle-income regions: A case of northwestern China. *Renew. Sustain. Energy Rev.* **2022**, *155*, 111942. [[CrossRef](#)]
13. Wang, P.P.; Zhao, Y.C.; Zhang, J.Y.; Xiong, Z. Progress of carbon measurement methods for coal-fired power plants under double carbon target. *Clean Coal Technol.* **2022**, *28*, 170–183. [[CrossRef](#)]
14. Gao, C.Y.; Niu, J.G.; Wang, F.R. Review of carbon emission accounting methods and carbon emission factor in steel production. *Contemp. Econ. Manag.* **2021**, *43*, 33–38. [[CrossRef](#)]
15. Jung, S.; An, K.-J.; Dodbiba, G.; Fujita, T. Regional energy-related carbon emission characteristics and potential mitigation in eco-industrial parks in South Korea: Logarithmic mean Divisia index analysis based on the Kaya identity. *Energy* **2012**, *46*, 231–241. [[CrossRef](#)]
16. Gregg, J.S.; Losey, L.M.; Andres, R.J.; Blasing, T.J.; Marland, G. The temporal and spatial distribution of carbon dioxide emissions from fossil-fuel use in North America. *J. Appl. Meteorol. Climatol.* **2009**, *48*, 2528–2542. [[CrossRef](#)]

17. Jorgenson, A.K.; Clark, B.; Giedraitis, V.R. The temporal (in)stability of the carbon dioxide emissions/economic development relationship in Central and Eastern European Nations. *Soc. Nat. Resour.* **2012**, *25*, 1182–1192. [[CrossRef](#)]
18. Shao, C.; Guan, Y.; Wan, Z.; Guo, C.; Chu, C.; Ju, M. Performance and decomposition analyses of carbon emissions from industrial energy consumption in Tianjin, China. *J. Clean. Prod.* **2014**, *64*, 590–601. [[CrossRef](#)]
19. Ouyang, X.; Lin, B. An analysis of the driving forces of energy-related carbon dioxide emissions in China's industrial sector. *Renew. Sustain. Energy Rev.* **2015**, *45*, 838–849. [[CrossRef](#)]
20. Ye, Y.; Yu, R.; Yu, Z.X. Study on industrial land use efficiency under energy carbon emission constraint. *J. Anhui Agric. Univ.* **2022**, *31*, 40–48. [[CrossRef](#)]
21. Wang, W.; Xie, H.L.; Jiang, T.; Zhang, D.B.; Xue, X. Measuring the Total-Factor Carbon Emission Performance of Industrial Land Use in China Based on the Global Directional Distance Function and Non-Radial Luenberger Productivity Index. *Sustainability* **2016**, *8*, 336. [[CrossRef](#)]
22. Xie, H.L.; Zhai, Q.L.; Wang, W.; Yu, J.L.; Lu, F.C.; Chen, Q.F. Does intensive land use promote a reduction in carbon emissions? Evidence from the Chinese industrial sector. *Resour. Conserv. Recycl.* **2018**, *137*, 167–176. [[CrossRef](#)]
23. Zeng, L.G.; Li, C.M.; Liang, Z.Q.; Zhao, X.H.; Hu, H.Y.; Wang, X. The carbon emission intensity of industrial land in China: spatiotemporal characteristics and driving factors. *Land* **2022**, *11*, 1156. [[CrossRef](#)]
24. Wu, S.; Hu, S.G.; Frazier, A.E. Spatiotemporal variation and driving factors of carbon emissions in three industrial land spaces in China from 1997 to 2016. *Technol. Forecast. Soc. Change* **2021**, *169*, 120837. [[CrossRef](#)]
25. Zhang, T.; Chen, L.Q.; Wang, R.; Wang, B.Y.; Liu, Y.Q.; Liu, W.Q.; Wang, J.; Wen, M.X. The influencing factors of industrial carbon emissions in the context of undertaking industrial transfer in Anhui Province, China. *Appl. Ecol. Environ. Res.* **2019**, *17*, 4205–4227. [[CrossRef](#)]
26. Dai, D.; Xing, Q. Low-carbon development forecast analysis of carbon emission in Anhui province (china). *Fresenius Environ. Bull.* **2022**, *31*, 3015–3022.
27. Xie, W.; Guo, W.; Shao, W.; Li, F.; Tang, Z. Environmental and health co-benefits of coal regulation under the carbon neutral target: A case study in Anhui Province, China. *Sustainability* **2021**, *13*, 6498. [[CrossRef](#)]
28. Ye, L.; Wu, X.; Huang, D. Industrial energy-related CO₂ emissions and their driving factors in the Yangtze River Economic Zone (China): An extended LMDI analysis from 2008 to 2016. *Int. J. Environ. Res. Public Health* **2020**, *17*, 5880. [[CrossRef](#)]
29. Tang, L.J.; Jiang, X.D.; Yang, Q.; Xu, X. Characteristics of carbon emission and its countermeasure during “13th Five-Year”. *J. Anhui Agric. Sci.* **2017**, *45*, 204–211. [[CrossRef](#)]
30. Hu, S.; Chen, L.; Li, L.; Zhang, T.; Yuan, L.; Cheng, L.; Wang, J.; Wen, M. Simulation of land use change and ecosystem service value dynamics under ecological constraints in Anhui Province, China. *Int. J. Environ. Res. Public Health* **2020**, *17*, 4228. [[CrossRef](#)]
31. Ghosh, S.; Dinda, S.; Das Chatterjee, N.; Dutta, S.; Bera, D. Spatial-explicit carbon emission-sequestration balance estimation and evaluation of emission susceptible zones in an Eastern Himalayan city using Pressure-Sensitivity-Resilience framework: An approach towards achieving low carbon cities. *J. Clean. Prod.* **2022**, *336*, 130417. [[CrossRef](#)]
32. Burns, D.; Grubert, E. Contribution of regionalized methane emissions to greenhouse gas intensity of natural gas-fired electricity and carbon capture in the United States. *Environ. Sci. Technol. Lett.* **2021**, *8*, 811–817. [[CrossRef](#)]
33. Yan, H.; Guo, X.; Zhao, S.; Yang, H. Variation of net carbon emissions from land use change in the Beijing-Tianjin-Hebei region during 1990–2020. *Land* **2022**, *11*, 997. [[CrossRef](#)]
34. Asiedu, B.A.; Hassan, A.A.; Bein, M.A. Renewable energy, non-renewable energy, and economic growth: Evidence from 26 European countries. *Environ. Sci. Pollut. Res.* **2021**, *28*, 11119–11128. [[CrossRef](#)]
35. Cang, D.; Chen, G.; Chen, Q.; Sui, L.; Cui, C. Does new energy consumption conducive to controlling fossil energy consumption and carbon emissions?—Evidence from China. *Resour. Policy* **2021**, *74*, 102427. [[CrossRef](#)]
36. Wei, W.; Zhang, X.; Cao, X.; Zhou, L.; Xie, B.; Zhou, J.; Li, C. Spatiotemporal dynamics of energy-related CO₂ emissions in China based on nighttime imagery and land use data. *Ecol. Indic.* **2021**, *131*, 108132. [[CrossRef](#)]
37. Ciais, P.; Wang, Y.; Andrew, R.; Breon, F.M.; Chevallier, F.; Broquet, G.; Nabuurs, G.J.; Peters, G.; McGrath, M.; Meng, W.; et al. Biofuel burning and human respiration bias on satellite estimates of fossil fuel CO₂ emissions. *Environ. Res. Lett.* **2020**, *15*, 074036. [[CrossRef](#)]
38. Rahman, M.M.; Sultana, N.; Velayutham, E. Renewable energy, energy intensity and carbon reduction: Experience of large emerging economies. *Renew. Energy* **2022**, *184*, 252–265. [[CrossRef](#)]
39. Zheng, X.; Yu, H.; Yang, L. Factor Mobility, Industrial transfer and industrial carbon emission: A spatial matching perspective. *Front. Environ. Sci.* **2022**, *10*, 822811. [[CrossRef](#)]
40. Zhang, Z.; Xie, H.; Zhang, J.; Wang, X.; Wei, J.; Quan, X. Prediction and trend analysis of regional industrial carbon emission in China: A study of Nanjing City. *Int. J. Environ. Res. Public Health* **2022**, *19*, 7165. [[CrossRef](#)]
41. Chen, H.; Qi, S.; Tan, X. Decomposition and prediction of China's carbon emission intensity towards carbon neutrality: From perspectives of national, regional and sectoral level. *Sci. Total Environ.* **2022**, *825*, 153839. [[CrossRef](#)] [[PubMed](#)]
42. Sun, W.; Huang, C. Predictions of carbon emission intensity based on factor analysis and an improved extreme learning machine from the perspective of carbon emission efficiency. *J. Clean. Prod.* **2022**, *338*, 130414. [[CrossRef](#)]
43. Zheng, Y.; Long, Y.; Fan, H. The analysis of spatial-temporal effects of relevant factors on carbon intensity in China. *Stoch. Environ. Res. Risk Assess.* **2022**, *36*, 3785–3802. [[CrossRef](#)] [[PubMed](#)]

44. Tian, H.Z.; Ma, L. Study on the change of China's industrial carbon emission intensity from the perspective of sector structure. *J. Nat. Resour.* **2020**, *35*, 639–653. [[CrossRef](#)]
45. Lin, B.; Xu, B. Growth of industrial CO₂ emissions in Shanghai City: Evidence from a dynamic vector auto regression analysis. *Energy* **2018**, *151*, 167–177. [[CrossRef](#)]
46. Shu, X.; Xia, C.Y.; Li, Y.; Tong, J.E.; Shi, Z. Relationships between carbon emission, urban growth and urban forms of urban agglomeration in the Yangtze River Delta. *Acta Ecol. Sin.* **2018**, *38*, 6302–6313. [[CrossRef](#)]
47. Lin, Q.W.; Zhang, L.; Qiu, B.K.; Zhao, Y.; Wei, C. Spatiotemporal analysis of land use patterns on carbon emissions in China. *Land* **2021**, *10*, 141. [[CrossRef](#)]
48. Peng, W.F.; Fan, S.Y.; Pan, H.J.; Mao, H.; Zhou, J.M.; Zhao, J.F.; Yang, C.J. Effects of region land use change on carbon emission and its spatial and temporal patterns, in Sichuan Province. *Ecol. Econ.* **2013**, *9*, 28–33.
49. Chen, Z.L.; Yihua; Lin, H. Decoupling analysis of land-use carbon emissions and economic development in Guangdong Province. *Ecol. Econ.* **2018**, *34*, 26–32.
50. Lefever, D.W. Measuring geographic concentration by means of the standard deviational ellipse. *Am. J. Sociol.* **1926**, *32*, 88–94. [[CrossRef](#)]
51. Wang, W.; Samat, A.; Abuduwaili, J.; Ge, Y. Spatio-temporal variations of satellite-based PM_{2.5} concentrations and its determinants in Xinjiang, Northwest of China. *Int. J. Environ. Res. Public Health* **2020**, *17*, 2157. [[CrossRef](#)] [[PubMed](#)]
52. Huang, J.; Song, L.; Yu, M.; Zhang, C.; Li, S.; Li, Z.; Geng, J.; Zhang, C. Quantitative spatial analysis of thermal infrared radiation temperature fields by the standard deviational ellipse method for the uniaxial loading of sandstone. *Infrared Phys. Technol.* **2022**, *123*, 104150. [[CrossRef](#)]
53. Wang, Y.; Song, J.; Zhang, X.; Sun, H. Sustainable development evaluation and its obstacle factors of the Weihe River Basin in Shaanxi Province, China. *Front. Earth Sci.* **2021**, *9*, 789. [[CrossRef](#)]
54. Zuo, Z.; Guo, H.; Cheng, J.; Li, Y. How to achieve new progress in ecological civilization construction?—Based on cloud model and coupling coordination degree model. *Ecol. Indic.* **2021**, *127*, 107789. [[CrossRef](#)]
55. Sun, D.; Hu, C.; Wang, Y.; Wang, Z.; Zhang, J. Examining spatio-temporal characteristics of urban heat islands and factors driving them in Hangzhou, China. *IEEE J. Sel. Top. Appl. Earth Obs. Remote Sens.* **2021**, *14*, 8316–8325. [[CrossRef](#)]
56. Cheng, L.; Zhang, T.; Chen, L.; Li, L.; Wang, S.; Hu, S.; Yuan, L.; Wang, J.; Wen, M. Investigating the impacts of urbanization on PM_{2.5} pollution in the Yangtze River Delta of China: A spatial panel data approach. *Atmosphere* **2020**, *11*, 1058. [[CrossRef](#)]
57. Li, H.; Li, L.; Chen, L.; Zhou, X.; Cui, Y.; Liu, Y.; Liu, W. Mapping and characterizing spatiotemporal dynamics of impervious surfaces using landsat images: A case study of Xuzhou, East China from 1995 to 2018. *Sustainability*. **2019**, *11*, 1224. [[CrossRef](#)]
58. Xia, C.; Hu, S.G.; Wu, S.; Yu, D. Spatial-temporal evolution characteristics of urban land use efficiency in Yangtze River Economic Belt. *Econ. Geogr.* **2021**, *41*, 115–124. [[CrossRef](#)]
59. Shu, B.R.; Li, Y.L.; Qu, Y.; Yong, X.Q.; Li, X. Urban land expansion and its driving forces in different functional Cities: An empirical analysis based on 137 cities in China. *J. Nanjing Agric. Univ.* **2014**, *14*, 86–92.
60. Shi, F.; Chu, J.L.; Gu, K.K. Construction of the central city group in Anhui Province based on spatial- Interaction theoretical perspective. *J. Shenyang Jianzhu Univ.* **2010**, *12*, 290–295.